Soft X-ray grating monochromators as a source of spatial coherence degradation: A wave-optical approach

Journal of Physics: Conference Series **2380** (2022) 012072 doi:10.1088/1742-6596/2380/1/012072

Soft X-ray grating monochromators as a source of spatial coherence degradation: A wave-optical approach

Ruslan Khubbutdinov, Martin Seyrich, Kai Bagschik

Deutsches Elektronen-Synchrotron (DESY), Notkestraße 85, 22607 Hamburg, Germany

E-mail: kai.bagschik@desy.de

Abstract. We present wave-optical simulations and a coherence analysis of the photon beam transported through a soft X-ray beamline, paying particular attention to a focusing varied line spacing (VLS) plane grating monochromator (PGM). We show that this beamline optical element used in several soft X-ray beamlines at synchrotron sources and free-electron lasers can cause a non-negligible spatial coherence degradation. We demonstrate that the origin of this effect arises from the coupling between spatial and spectral properties of the photon beam generated by the grating. The latter implies that space and frequency dependencies are not separable after such a dispersive element. It is shown which parameters are essential for this effect and how they are linked to each other.

1. Introduction

Existing and future diffraction-limited storage rings promise an enormous enhancement of the spatial coherence properties of the photon source by reducing the electron emittance [1–4]. This is particularly evident in the energy range of hard and high-energy X-rays. In the soft X-ray range, most existing sources are already diffraction limited, at least in the vertical direction. However, in this photon energy range, diffraction-limited storage rings are expected to achieve a spatial degree of coherence of the total beam of nearly 100% and thus resemble a laser source in terms of spatial coherence. In this case, the photon flux of the source can be considered completely coherent, and thus, the spatial degree of coherence does not need to be increased by, e. g., slit systems at the expense of flux. These beam properties not only bring new scientific opportunities, but also pose enormous challenges for the optical layout of the beamlines and the quality of the optics used. The high spatial coherence of the source must be preserved by the photon beam transport system to make it available for the actual experiment at the end of the beamline. It has already been demonstrated that the spatial coherence degradation of the source may occur, e. g., due to optical surface defects [5–8], incoherent scattering [9, 10], or vibrations of optical elements [11–13]. The latter effect imposes the most significant influence on the spatial coherence so far. This becomes obvious with modern beamline designs and their use of almost exclusively horizontally deflecting optics, which are less susceptible to vibrations.

One way to reproduce experimental measurements or identify the phenomena of spatial coherence degradation and clarify their cause, is through wave-optical simulations [14, 15]. Wave-optical simulations allow to explore various beamline design options including real optical

surfaces, vibrations, misalignments and many other aspects. Almost every simulation tool that offers wave-optical calculations also has built-in tools to determine the spatial coherence properties from the obtained wave fields. Many of the coherence analysis tools can also be integrated in existing wave-optical simulation software or the coherence can be calculated externally using the obtained wave fields. The presented results are based on wave-optical simulations with slightly polychromatic light using the software Xrt [14] and are supported by experimental observations [13, 16, 17]. In the following, we present that the soft X-ray focussing variable line spacing plane grating monochromator (VLS-PGM) used in many soft X-ray beamlines is a source of spatial coherence degradation and can cause a huge drop in spatial coherence. Here, we describe the effect of the spatial coherence degradation by the monochromator and show which parameters are decisive for it and what are the dependencies.

2. Beamline layout and focusing VLS-PGM

The beamline layout used for the wave-optical simulations is based on the layout of the P04 beamline at PETRA III [18] (see figure 1). The insertion device is an APPLE-II undulator, which delivers photon energies in the range of $E = 250 - 3000$ eV in the first harmonic. The first element of the beamline is a beam-defining aperture which is located 27.9 m downstream from the source. It serves as an angular filter and increases the spatial coherence when the aperture is closed. The monochromator is a focusing VLS-PGM and consists of a plane mirror, a variable line spacing (VLS) plane grating and an exit slit unit (EXSU). The monochromator is located 46 m downstream from the source. The VLS plane grating spectrally splits the photon beam due to angular dispersion. Due to the variable line spacing of the grating, the photon beam is additionally focused on the exit slit in the vertical direction, which is located 25 m behind the grating. The exit slit selects a certain bandwidth and defines the energy resolution of the monochromator. The plane mirror in front of the grating illuminates the grating at an angle of incidence that simultaneously satisfies the grating equation $nk\lambda = \sin\alpha + \sin\beta$ and the focusing condition of the plane grating $\cos\beta/\cos\alpha = c_{ff}$ [19]. The angles α and β are the angles of incidence and diffraction, n is the diffraction order, λ is the wavelength, k is the line density, and c_{ff} is the fixed focus constant. When scanning the photon energy with the monochromator, c_{ff} is kept constant, resulting in exact focusing with fixed entrance r and exit arm length r'. The magnification of the VLS grating is defined by [20]:

$$M = \frac{r'}{r \cdot c_{ff}} \tag{1}$$

Using the distances shown in figure 1 and described above, and a $c_{ff} = 2.0$ (PETRA III beamline P04, $k = 1200$ l/mm grating), the source is demagnified with $M = 0.27$ onto the exit slit. Due to the angular dispersion of the grating, the photon beam of each wavelength is focused individually at a different z-positions along the exit slit (see figure 1). Due to the finite resolution function of the monochromator and the finite photon beam size for each wavelength, the individual photon beams also overlap, representing the angular dispersion function of the grating. The spatial extend of the dispersed photon beam at the exit slit position can be determined by the reciprocal linear dispersion $\Delta\lambda/\Delta z$ [21] and the bandwidth of the illuminating photon beam ΔE and is given by:

$$\Delta z[mm] = \frac{1.24 \cdot 10^{-3} \cdot nkr'[m]}{\cos\beta \cdot E^2[eV]} \Delta E[eV] \tag{2}$$

A photon beam incident on the VLS grating with a photon energy of $E = 1200$ eV and an energy bandwidth of $\Delta E = 200$ meV will generate a beam profile with a size of $\Delta z = 89$ μm (FWHM) at the exit slit position.

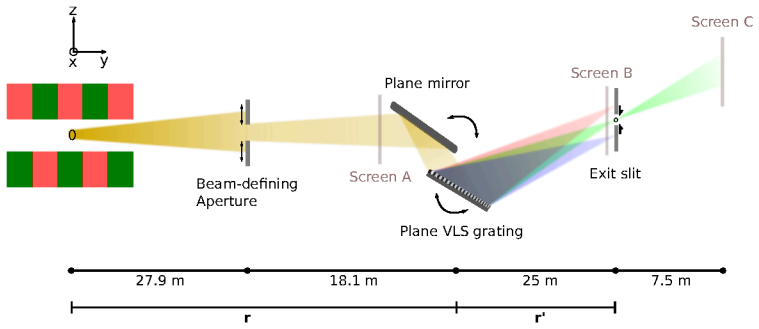

Figure 1. Beamline Layout used for the wave-optical simulations. The coherence analysis of the wave fields using the standard methods and the CMD is performed at screen A after the beam-defining aperture, at screen B closely before the exit slit, and at screen C after the exit slit.

3. Wave-optical simulations

For the wave-optical simulations we used the software Xrt [14]. For efficiency and performance reasons, a filament electron beam with zero energy spread was used as the source of radiation which means that the photon source is characterised only by the intrinsic properties of a single electron. Such a photon source has a spatial degree of coherence of $\zeta = 100\%$. The photon energy has been set to $E = 1200$ eV for all simulations. Furthermore, the size of the beam-defining aperture was chosen to be 50 μm x 400 μm (h x v). In addition, a horizontal size of 50 μm was set for the exit slit.

Assuming that the statistical process is stationary, the calculation of the spatial coherence is based on the standard methods [22] and the use of the coherent mode decomposition (CMD) [23]. As a result, one obtains the spatial degree of coherence ζ and the coherent fraction (CF) of the investigated wave fields. Both are single values that represent the spatial coherence properties of the total beam. The photon beam energy bandwidth ΔE used for the simulations was selected such that the quasi-monochromatic approximation can be applied for the coherence analysis methods, which is the case if $\Delta E \ll E$ [22, 23]. In the simulations, it was ensured that the number of electrons used lead to reasonable statistics where the obtained spatial coherence values converge and does not change anymore with increasing number of electrons. The number of modes was chosen such that the cumulative sum of the mode weights always equals one. These two facts lead to reliable coherence values for the presented simulations.

4. Results and discussion

To analyse the spatial coherence properties of the photon beam along the beamline and thus the influence of the VLS plane grating monochromator on the spatial coherence properties, the spatial degree of coherence ζ was determined at three different positions. The first position (screen A) has been set after the beam-defining aperture and closely before the plane mirror, the second position (screen B) is after the grating and closely before the exit slit, and the third position (screen C) is after the exit slit (see figure 1). As mentioned in the previous section, the source generates a fully coherent beam with a spatial degree of coherence of $\zeta = 100\%$. In case of a monochromatic source with just a single photon energy $E = 1200$ eV, the VLS grating monochromator generates a focused beam at the exit slit position with a size of $\sigma_b = 7$ μm (rms) based on the magnification described in equation (1). The exit slit size was set to $w_e = 20$ μm in this case. The spatial degree of coherence of the photon beam at screen A, B, and C is $\zeta = 100\%$, as expected. The exit slit size is larger than the beam size at the exit slit and therefore has no effect on the beam size or spatial coherence after the exit slit.

The same analysis was performed for a polychromatic source with a very narrow photon energy bandwidth of $\Delta E = 200$ meV. This bandwidth results in an energy resolution of $\Delta E/E = 1.6 \cdot 10^{-4}$ at 1200 eV so that the quasi-monochromatic approximation can be applied for the coherence analysis methods. We found that at a finite bandwidth of $\Delta E = 200$ meV, the

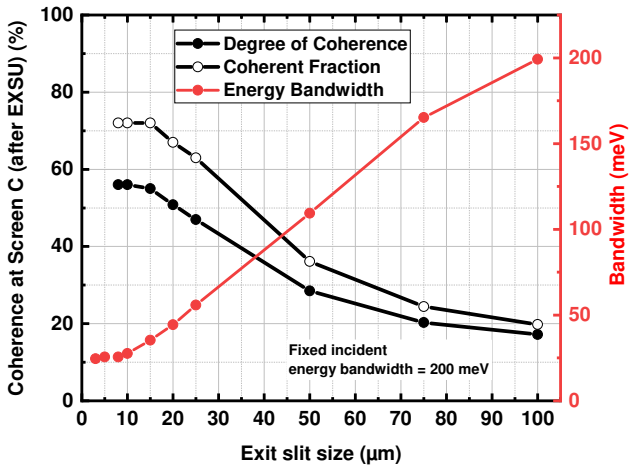

Figure 2. Spatial degree of coherence and coherent fraction at screen C for different exit slit sizes. The corresponding energy bandwidth at screen C is indicated in red. The incident energy bandwidth has been set to $\Delta E = 200$ meV.

beam at the source and at screen A still has a spatial degree of coherence of $\zeta = 100\%$, this is also true for all bandwidths below $\Delta E = 600$ meV. In this case and at these positions, the spatial coherence properties of the photon beam is therefore decoupled from the spectral properties of the beam, which is to be expected. The photon beam size after the grating is determined by ΔE incident on the grating as described in equation (2). Hence, at screen position B spatial and spectral properties are correlated to some extent. When analysing the coherence properties of the photon beam at screen B, we found that the degree of spatial coherence drops significantly to $\zeta = 17\%$ (at $\Delta E = 200$ meV). This is at first glance a very surprising and unexpected result, since the photon beam at this position is a superposition of several fully coherent single Gaussian beams whose spacing is determined by the dispersion properties of the grating. We further analysed the coherence properties after the exit slit at screen C to investigate the effect of the slit on the spatial coherence properties of this beam. For this, the slit size was varied between $w_e = 100$ μm and 8 μm and the spatial degree of coherence of the photon beam at screen C was determined (see figure 2). We found that the spatial degree of coherence increases with decreasing slit size, which is an expected result considering the coherence properties of the incident beam. The obtained results are in line with several independent experimental findings which also describe that the assumed fully coherent beam of the source at soft X-ray beamlines in the vertical direction show a rather low spatial degree of coherence in this direction and that it can be increased or decreased with closing or opening the exit slit, respectively [13, 16, 17]. The experimental findings thus support the results of the simulations. Starting from an exit slit size of around $w_e = 20$ μm and going towards smaller exit slit sizes, we see an effect which is opposite to the expected behaviour. Below an exit slit size of $w_e = 20$ μm, the degree of spatial coherence saturates to $\zeta = 56\%$ and remains constant with decreasing exit slit size. Looking at the transmitted ΔE, we see the same effect. The photon energy bandwidth even remains constant with $\Delta E = 25$ meV. In terms of ΔE, this is an expected behaviour since the minimum photon energy bandwidth achieved is determined by the dispersion properties of the grating and cannot be further reduced by closing the exit slit. The observed phenomena lead to the assumptions that there is a strong correlation between the spatial coherence properties and the spectral properties of the photon beam after the grating, similar to the spatial dimensions as described in equation (2).

To explore this effect in more detail and to determine its dependencies, we set a fixed exit slit size of $w_e = 20$ μm and varied ΔE of the source (see figure 3). In figure 3(a), we compare the degree of spatial coherence at screen B and screen C as a function of ΔE. Figure 3(b) shows

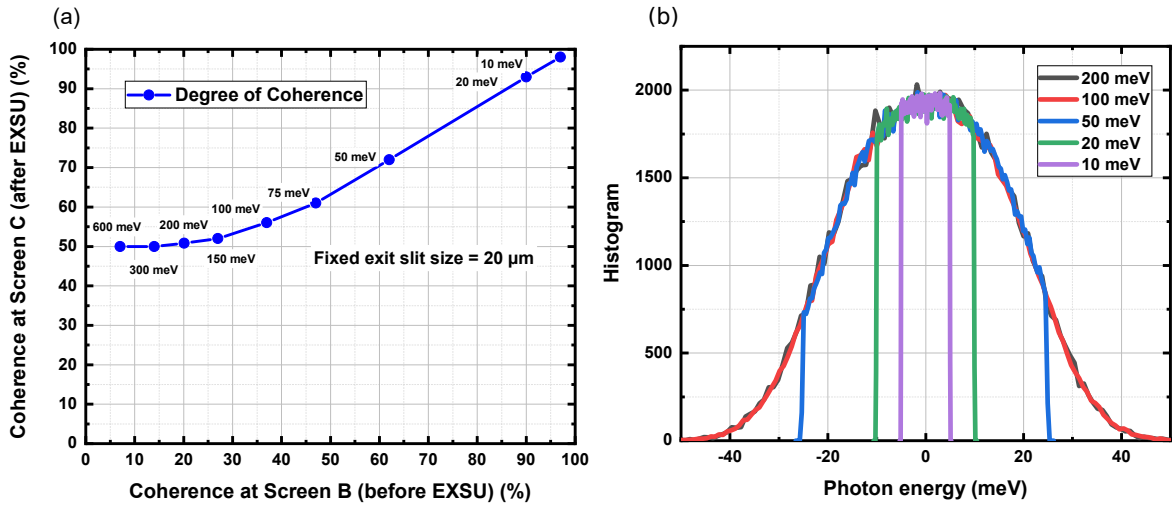

Figure 3. (a) Comparison of the obtained spatial degree of coherence between the photon beam incident on the exit slit (screen B) and the photon beam after the exit slit (screen C) for different incident photon energy bandwidths (ΔE = 10 meV - 600 meV). The exit slit size has been set to $w_e = 20$ μm. (b) Spectrum of the photon beam at screen C for a set of five different incident photon energy bandwidths.

the transmitted photon energy bandwidth at screen C as a function of the incident photon energy bandwidth at screen B. We found, that in case of $\Delta E = 10$ meV and $\Delta E = 20$ meV, the spatial degree of coherence is similar to the monochromatic case. The photon beam, in this case, is smaller than the 20 μm exit slit size and hence even the photon energy bandwidth of the incoming and transmitted beam is the same. At $\Delta E = 50$ meV the size of the photon beam incident on the exit slit is slightly larger than the exit slit size. The transmitted photon energy bandwidth is even slightly smaller than the incoming one. In this case, the degree of spatial coherence of the incoming and transmitted beam is different. After the exit slit the spatial degree of coherence is about 10% larger. With increasing ΔE, we found that the degree of spatial coherence determined at screen C converges to $\zeta = 50\%$ and does not further decrease whereby the degree of spatial coherence at screen B further decreases. We see that this happens exactly at the point where the transmitted $\Delta E = 44$ meV does not change anymore due to the finite bandpass of the 20 μm exit slit size.

5. Conclusion

The conclusion from the simulations and the obtained results is that due to the dispersive properties of the grating, the spatial coherence properties of the photon beam after the grating are coupled with its spectral properties and exhibit a certain dependency. The spatio-frequency coupling is caused by the spatial redistribution of different wavelength by the grating. Photon beams with different wavelengths still overlap at the exit slit position. The degree of overlap is determined by the size of the individual photon beams of each wavelength and their separation defined by the grating. In the decoupled state, as it is the case upstream of the grating before dispersion occurs, the degree of spatial coherence is unaffected. Hence, we assume that the spatio-frequency coupling is the root cause of the spatial coherence degradation. Caution is advised when the photon bandwidth becomes so large that the quasi-monochromatic approximation no longer applies and the temporal coherence properties affect the spatial coherence properties. We have found that the degree of spatial coherence after the exit slit

is mainly determined by the bandpass and thus the angular dispersion of the grating if a large photon beam (large energy bandwidth) is incident on the exit slit, which is the case at the beamline. Thus, due to this dependence, the transmitted beam is to a large extent independent of the spatial coherence of the incident beam. Nevertheless, the simulated data show that the VLS plane grating monochromator can lead to a non-negligible spatial coherence degradation. The effect of spatial coherence degradation of the photon beam in the dispersive direction was experimentally observed utilizing first [13, 16, 17] and second order correlation theory [24]. Further simulations with varying photon energies and grating parameters can be performed to find out to what extent this effect can be mitigated to ensure an optimal coherent flux even for highly-coherent radiation sources. More details will follow in a forthcoming paper.

Acknowledgments

We would like to thank Ivan Vartaniants and Evgeny Saldin for very helpful and deep discussions about coherence theory. This research was supported in part through the Maxwell computational resources operated at Deutsches Elektronen-Synchrotron DESY, Hamburg, Germany.

References

[1] Schroer C G, Agapov I, Brefeld W, Brinkmann R, Chae Y-C , Chao H-C, Eriksson M, Keil J, Nuel Gavalda X, Röhlsberger R, Seeck O H, Sprung M, Tischer M, Wanzenberg R and Weckert E 2018 *J. Synchrotron Radiat.* **25** 1277
[2] Steier C 2014 *Synchrotron Radiat. News* **27** 18
[3] Raimondi P 2016 *Synchrotron Radiat. News* **29** 8
[4] Tavares P F, Leemann S C, Sjöström M and Andersson A 2014 *J. Synchrotron Radiat.* **21** 862
[5] Siewert F, Buchheim J, Zeschke T, Störmer M, Falkenberg G and Sankari R 2014 *J. Synchrotron Radiat.* **21** 968
[6] Yabashi M, Tono K, Mimura H, Matsuyama S, Yamauchi K, Tanaka T, Tanaka H, Tamasaku K, Ohashi H, Goto S and Ishikawa T 2014 *J. Synchrotron Radiat.* **21** 976
[7] Wang Y, Xiao T and Xu H 2000 *J. Synchrotron Radiat.* **7** 209
[8] Meng X, Shi X, Wang Y, Reininger R, Assoufid L and Tai R 2017 *J. Synchrotron Radiat.* **24** 954
[9] Cheng C-C and Raymer M G 2000 *Phys. Rev A* **62** 023811
[10] Robinson I K, Kenney-Benson C A and Vartanyants I A 2003 *Phys. B* **336** 56
[11] Grizolli W, Shi X and Assoufid L 2019 *Opt. Lett.* **44** 899
[12] Goto S 2015 *Proc. SPIE* **9588** 95880G
[13] Bagschik K, Wagner J, Buß R, Riepp M, Philippi-Kobs A, Müller L, Buck J, Trinter F, Scholz F, Seltmann J, Hoesch M, Viefhaus J, Grübel G, Oepen H P and Frömter R 2020 *Opt. Express* **28** 7282
[14] Klementiev K and Chernikov R 2014 *Proc. SPIE* **9209** 92090A
[15] Chubar O, Chu Y S, Kaznatcheev K and Yan H 2011 *Nucl. Instrum. Methods Phys. Res., Sect. A* **649** 118
[16] Skopintsev P, Singer A, Bach J, Müller L, Beyersdorff B, Schleitzer S, Gorobtsov O, Shabalin A, Kurta R P, Dzhigaev D, Yefanov O M, Glaser L, Sakdinawat A, Grübel G, Frömter R, Oepen H P, Viefhaus J and I A Vartanyants, 2014 *J. Synchrotron Radiat.* **21** 722
[17] Rose M, Skopintsev P, Dzhigaev D, Gorobtsov O, Senkbeil T, von Gundlach A, Gorniak T, Shabalin A, Viefhaus J, Rosenhahn A and Vartanyants I A 2015 *J. Synchrotron Radiat.* **22** 819
[18] Viefhaus J, Scholz F, Deinert S, Glaser L, Ilchen M, Seltmann J, Walter P and Siewert F 2013 *Nucl. Instrum. Methods Phys. Res., Sect. A* **710** 151
[19] Reininger R 2011 *Nucl. Instrum. Methods Phys. Res., Sect. A* **649** 139
[20] Peatman W B 1997 Gratings, Mirrors and Slits: Beamline Design for Soft X-ray Synchrotron Radiation Sources (Gordon & Breach New York) chapter 4 pp 91-111
[21] Thompson A C and Vaughan D 2001 X-ray Data Booklet (Lawrence Berkeley National Laboratory USA) section 4.3
[22] Mandel L and Wolf E 1995 Optical Coherence and Quantum Optics *Cambridge University Press*
[23] Khubbutdinov R, Menushenkov A P and Vartanyants I A 2019 *J. Synchrotron Radiat.* **26** 1851
[24] Khubbutdinov R, Gerasimova N, Mercurio G, Assalauova D, Carnis J, Gelisio L, Le Guyader L, Ignatenko A, Kim Y Y, Van Kuiken B E, Kurta R P Lapkin D, Teichmann M, Yaroslavtsev A, Gorobtsov O, Menushenkov A P, Scholz M, Scherz A, and Vartanyants I A 2021 *Struct. Dyn.* **8** 044305